



Magnetic Features of Spin-1 One-Dimensional Ising System

Gökçen DİKİCİ YILDIZ*

*Kırıkkale University, Faculty of Art and Sciences, Department of Physics, 71450, Kırıkkale,
Turkey

*corresponding author e-mail: gkcndkc@kku.edu.tr

(Received: 22.04.2019, Accepted: 10.05.2019, Yayınlanma / Published: 31.05.2019)

Abstract: In this work, we investigated the temperature and applied field dependence of the magnetization and quadrupolar moment of the spin-1 one-dimensional Ising system (S1-1DIS) by using Kaneyoshi approach throughout the Effective Field Theory (EFT). We determined that the S1-1DIS has a first or second order phase transition according to the crystal field, the magnetization of the S1-1DIS has a second-order phase transition for $D=0$ whereas the quadrupolar moment has no phase transition at T_c . The magnetization of the S1-1DIS has a first-order phase transition for $D = -2.6$ at T_f but the quadrupolar moment has phase transition at T_f and it increases at $T \geq T_f$, paramagnetic magnetic susceptibility decreases monotonically at $T \geq T_c$ whereas it has a broad maximum at $T \geq T_f$. Because of the $M_T=0.0$ at $T \geq T_c$ and T_f , it can be concluded that susceptibility behaviors in the paramagnetic region result from the quadrupolar moment. On the other hand, the slope of the hysteresis curves of the M_T decreases as the temperature increases and they become zero at high temperature. The theoretical first-order phase transition result of the S1-1DIS is the confirmation of the result of KH_2PO_4 (KPD) firstly reported by Kittel that one-dimensional system of the KPD undergoes a first-order phase transition at $T \neq 0$.

Keywords: One-dimensional Ising system, Magnetization, Effective field theory, Phase transition.

Spin-1 Tek Boyutlu Ising Sisteminin Manyetik Özellikleri

Özet: Bu çalışmada, etkin alan teorisinde Kaneyoshi yaklaşımı kullanarak tek boyutlu Ising sisteminin (S1-1DIS) spin-1'in sıcaklık ve dış manyetik alana bağlı mıknatıslanma ve kuadrupol momenti araştırıldı. S1-1DIS'in kristal alanına göre birinci veya ikinci dereceden bir faz geçişine sahip olduğu; S1-1DIS'in mıknatıslanmasının $D = 0$ için ikinci dereceden bir faz geçişine sahip olduğu; ancak kuadrupolar momentin T_c 'de faz geçişine sahip olmadığı belirlendi. S1-1DIS' in mıknatıslanması, T_f ' de $D = -2.6$ için birinci dereceden bir faz geçişine sahiptir, ancak kuadrupolar moment T_f ve $T > T_f$ ' de artarken faz geçişine sahiptir; paramanyetik manyetik alınganlık, $T > T_c$ 'de monotonik olarak azalır, oysa $T > T_f$ ' de geniş bir maksimuma sahiptir. $T > T_c$ ve T_f 'deki $M_T = 0.0$ nedeniyle, paramanyetik bölgedeki alınganlık davranışlarının kuadrupolar momentten kaynaklandığı sonucuna varılabilir. Diğer taraftan, M_T ' nin histerezis eğrilerinin eğimi, sıcaklık arttıkça azalır ve yüksek sıcaklıkta sıfır olur. S1-1DIS'in birinci dereceden faz geçişinin teorik sonucu, ilk olarak Kittel tarafından bildirilen KH_2PO_4 'ün (KPD) bir boyutlu sisteminin $T \neq 0$ da birinci dereceden bir faz geçişine uğradığı sonucunun teyididir.

Anahtar kelimeler: Tek boyutlu Ising sistem, Mıknatıslanma, Etkin alan teorisi, Faz geçişi.

1. Introduction

Recently, the EFT developed by Kaneyoshi has been used in the theoretical investigation of the magnetic features of the nanostructures [1-20], due to the description of the low-dimensional systems is very easily applied by using EFT and the theoretical results of that system obtained by EFT are in good consistent with the other theoretical and experimental findings of low-dimensional systems. Such as, magnetic features of the Ising nanowire [21-32], core/shell Ising nanostructures [33-35], Ising nanotube [36,37], Ising thin film [38], Ising nanolattices [39], Ising nanographene [40] and one-dimensional Ising system (1DIS) [41] were worked by using effective field theory. Although the EFT is commonly widely used for the examinations of the magnetic features of the low-dimensional system and its theoretical findings are in good consistent with the experimental results of that system, there is only one work reported by Şarlı [41]. In this work, magnetic features of the spin-1/2 1DIS were investigated and showed that the magnetic features of the 1DIS depend on the next-nearest neighbor exchange interaction. However, these features of the spin-1 1DIS have not been examined yet. Therefore, we aim to investigate the magnetic features of the spin-1 one-dimensional Ising system (S1-1DIS). Such as, crystal field effects on the magnetization; magnetic susceptibility, quadrupolar moment, quadrupolar susceptibility, their temperature and applied field depend on the S1-1DIS by using Kaneyoshi approach within the EFT.

On the other hand, one-dimensional systems are investigated by using different models. Such as transfer-matrix method [42], Jordan–Wigner transformation [43], random fields Ising model [44], Glauber dynamics of 1D nearest neighbor Ising model and 1D axial next-nearest neighbor Ising model [45], 1D sine-Gordon model [46], Chui-Week’s model [47], Burkhardt’s model [48], Dauxois-Peyrard’s model [49, 50], Van Hove’s theorem [51-54] and Landau and Lifshitz’s argument [55]. Our theoretical results of the first-and second order phase transition in the S1-1DIS with the next-nearest neighbor exchange interaction show that the one-dimensional system has firstand second order phase transition at $T \neq 0$. Especially, our theoretical first-order phase transition result of the S1-1DIS is in good agreement with the result of KH₂PO₄ (KPD) firstly reported by Kittel that one-dimensional system of the KPD undergoes a first-order phase transition at $T \neq 0$ [56].

2. Theoretical Method

We search for the magnetic features of the ferromagnetic ($J_1 > 0$) S1-1DIS shown in Figure 1 [41] in which each site is occupied by the spin-1 Ising particle. By using Kaneyoshi approach [1-20], the Hamiltonian of the S1-1DIS is given by,

$$\mathcal{H} = -J_1 \sum_{\langle i,j \rangle} S_i^z S_j^z - J_2 \sum_{\langle\langle i,j \rangle\rangle} S_i^z S_j^z - D \left(\sum_i (S_i^z)^2 + \sum_j (S_j^z)^2 \right) - H \left(\sum_i S_i^z + \sum_j S_j^z \right). \quad (1)$$

Where, J_1 is the exchange interaction between two nearest-neighbor magnetic atoms (m_1 and m_2) of the S1-1DIS. J_2 is the exchange interaction between two next nearest-neighbor magnetic atoms (m_1 and m_1 or m_2 and m_2) of the S1-1DIS. $S^z = \pm 1, 0$ is the Pauli spin operator. H is the external magnetic field. D is the crystal field. The S1-1DIS shown in Figure 1 has two unsimilar magnetizations; m_1 and m_2 are the magnetization of the S1-1DIS. m_1 and m_2 are the nearest-neighbor atoms and they interact with the nearest-neighbor exchange interaction J_1 . m_1 and m_1 or m_2 and m_2 interact with the next nearest-neighbor exchange interaction J_2 . One notes the next nearest-neighbor exchange interaction (J_2) should be small than the nearest-neighbor exchange interaction ($J_2 < J_1$,

for our calculations $J_2=0.9 < J_1=1$). The magnetizations (m_1 and m_2) and the quadrupolar moments ($q_i=m_i^2$, q_1 and q_2) of the S1-1DIS are given by as follows,

$$\begin{aligned}
m_1 &= \left[1 + m_1 \sinh(J_2 \nabla) + q_1 (\cosh(J_2 \nabla) - 1) \right]^2 \\
&\quad \left[1 + m_2 \sinh(J_1 \nabla) + q_2 (\cosh(J_1 \nabla) - 1) \right]^2 F_{S-1}(x) \Big|_{x=0}, \\
m_2 &= \left[1 + m_1 \sinh(J_1 \nabla) + q_1 (\cosh(J_1 \nabla) - 1) \right]^2 \\
&\quad \left[1 + m_2 \sinh(J_2 \nabla) + q_2 (\cosh(J_2 \nabla) - 1) \right]^2 F_{S-1}(x) \Big|_{x=0}, \\
q_1 &= \left[1 + m_1 \sinh(J_2 \nabla) + q_1 (\cosh(J_2 \nabla) - 1) \right]^2 \\
&\quad \left[1 + m_2 \sinh(J_1 \nabla) + q_2 (\cosh(J_1 \nabla) - 1) \right]^2 G_{S-1}(x) \Big|_{x=0}, \\
q_2 &= \left[1 + m_1 \sinh(J_1 \nabla) + q_1 (\cosh(J_1 \nabla) - 1) \right]^2 \\
&\quad \left[1 + m_2 \sinh(J_2 \nabla) + q_2 (\cosh(J_2 \nabla) - 1) \right]^2 G_{S-1}(x) \Big|_{x=0}.
\end{aligned} \tag{2}$$

where, $\nabla = \partial / \partial x$ is the differential operator and the function of $F_{S-1}(x)$ and $G_{S-1}(x)$ are determined by as follows for the spin-1 Ising particles.

$$\begin{aligned}
F_{S-1}(x) &= \frac{2 \text{Sinh}[\beta(x+H)]}{2 \text{Cosh}[\beta(x+H)] + \text{Exp}[-\beta D]}, \\
G_{S-1}(x) &= \frac{2 \text{Cosh}[\beta(x+H)]}{2 \text{Cosh}[\beta(x+H)] + \text{Exp}[-\beta D]}.
\end{aligned} \tag{3}$$

According to the Kaneyoshi approach (KA) [1-20] on the magnetic features of the nanostructure within the EFT, the magnetizations and S1-1DIS' susceptibility are obtained as in Eq. (2). From Eq. (2) and Eq.(4) [57], the magnetizations of the S1-1DIS are obtained as follows,

$$e^{a\nabla} = f(x+a). \tag{4}$$

$$\begin{aligned}
m_i &= (A_0 + A_1 m_i + A_2 q_i + A_3 m_i q_i + \dots) F_{\text{Spin-1}}(x) \Big|_{x=0}, \\
q_i &= (A_0 + A_1 m_i + A_2 q_i + A_3 m_i q_i + \dots) G_{\text{Spin-1}}(x) \Big|_{x=0}.
\end{aligned} \tag{5}$$

By distinguishing each side of the Eq. (5) with H, we gain the susceptibilities (χ) of the S1-1DIS as follows,

$$\begin{aligned}
\chi_{m_i} &= \lim_{H \rightarrow 0} \frac{\partial m_i}{\partial H}, \\
\chi_{q_i} &= \lim_{H \rightarrow 0} \frac{\partial q_i}{\partial H}.
\end{aligned} \tag{6}$$

by using Eqs. (5) and (6), we obtain the χ_{m1} , χ_{m2} , χ_{q1} and χ_{q2} as follows,

$$\begin{aligned}
\chi_{m1} &= a_1\chi_{m1} + a_2\chi_{m2} + a_0 \frac{\partial}{\partial H} F_{\text{Spin-1}}(x) \Big|_{x=0}, \\
\chi_{m2} &= b_1\chi_{m1} + b_2\chi_{m2} + b_0 \frac{\partial}{\partial H} F_{\text{Spin-1}}(x) \Big|_{x=0}, \\
\chi_{q1} &= c_1\chi_{q1} + c_2\chi_{q2} + c_0 \frac{\partial}{\partial H} G_{\text{Spin-1}}(x) \Big|_{x=0}, \\
\chi_{q2} &= d_1\chi_{q1} + d_2\chi_{q2} + d_0 \frac{\partial}{\partial H} G_{\text{Spin-1}}(x) \Big|_{x=0}.
\end{aligned} \tag{7}$$

Where, the coefficients a_i , b_i , c_i and d_i ($i=0, 1, 2$) are very long expressions. After having the solution Eq. (7) numerically and inputting the values into Eq.(8), we obtain the M_T , Q_T , χ_{MT} and χ_{QT} of the S1-1DIS follows,

$$\begin{aligned}
M_T &= \frac{1}{2}(m_1 + m_2), \\
Q_T &= \frac{1}{2}(q_1 + q_2), \\
\chi_{MT} &= \frac{1}{2}(\chi_{m1} + \chi_{m2}), \\
\chi_{QT} &= \frac{1}{2}(\chi_{q1} + \chi_{q2}).
\end{aligned} \tag{8}$$

3. Results and Discussion

First, we regarded the temperature dependence of the total magnetization (M_T), total quadrupolar moment (Q_T), total magnetic susceptibility (χ_{MT}) and total quadrupolar susceptibility (χ_{QT}) of the ferromagnetic ($0 < J_1$) S1-1DIS shown in Figure 1 [41].

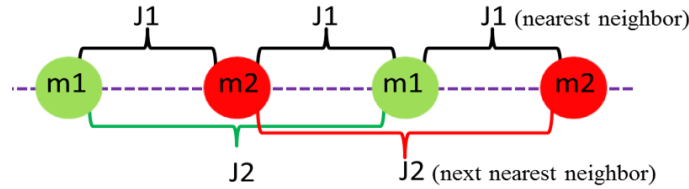


Figure1. The one-dimensional Ising system (1DIS) [41].

Our calculations show that the nearest-neighbor exchange interaction is $J_1=1$ and the next nearest-neighbor exchange interaction values should be smaller than the nearest-neighbor exchange interaction value is $J_2=0.9$ (It should be $J_2 < J_1$). Figure 2 indicates the temperature dependence of the total magnetization (M_T), total quadrupolar moment (Q_T), total magnetic susceptibility (χ_{MT}) and total quadrupolar susceptibility (χ_{QT}) of the ferromagnetic ($0 < J_1$) S1-1DIS for the crystal field is $D=0$. The total magnetization of the FM S1-1DIS is indicated in Figure 2(a1). The second-order phase transition from ferromagnetic phase to paramagnetic phase occurs at $T_c=1.532J/k_B$. According to the Şarlı's study, coercive field point, remanent magnetization and the area of the hysteresis loop of the 1DIS decreases as the J_2 decreases, the hysteresis curves of the 1DIS exhibit paramagnetic hysteresis behavior for small J_2 in the ferromagnetic case. The total magnetization is $M_T=1$ at $T=0$. In Figure 2(a2), the total magnetic susceptibility of the FM S1-1DIS has reached a marked peak at T_c and monotonously decreases in the paramagnetic region ($T > T_c$). The total quadrupolar moment of the FM S1-1DIS is shown in Figure 2(b1). The total quadrupolar moment of the FM S1-1DIS decreases as the temperature increases until $T_c=1.532J/k_B$ and it has small changes at high temperature ($T \gg T_c$). One notes that total quadrupolar moment has no phase transition

and doesn't become zero whereas the total magnetization becomes zero at $T \geq T_c$. The total quadrupolar moment is $Q_T=1$ at $T=0$ and it is $Q_T=0.786$ at T_c . The total quadrupolar susceptibility of the FM S1-1DIS has a maximum as the temperature approaches to T_c and becomes zero at $T \geq T_c$. One notes that the paramagnetic magnetic susceptibility behavior in the paramagnetic region results from the quadrupolar moment (Q_T). Because of the total magnetization (M_T) and the external magnetic field (H) are zero at $T \geq T_c$. Similarly, quadrupolar susceptibility behavior in the paramagnetic region results from the magnetization (M_T). Because of the total magnetization (M_T) is zero at $T \geq T_c$. The theoretical second-order phase transition and susceptibility results of the S1-1DIS agrees with the results low-dimensional magnets reported by Balanda [58].

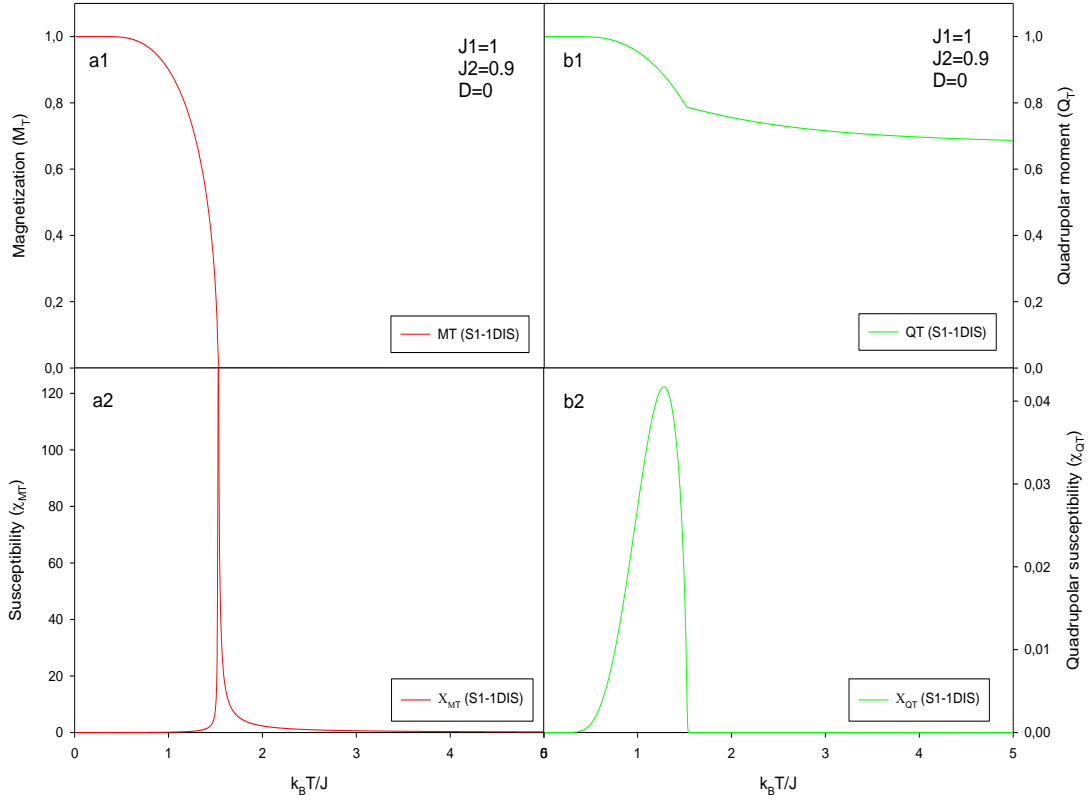


Figure 2. The temperature dependence of the magnetization (a1), susceptibility (a2), quadrupolar moment (b1) and quadrupolar susceptibility (b2) of the S1-1DIS for $J_1=1$, $J_2=0.9$ and $D=0$.

By Figure 3, the temperature dependence of the M_T , Q_T , χ_{MT} and χ_{QT} of the FM S1-1DIS for the crystal field is $D=-2.6$. The M_T of the FM S1-1DIS is shown in Figure 3(a1). The first-order phase transition from ferromagnetic phase to paramagnetic phase occurs at $T_f=0.281J/k_B$. The total magnetization is $M_T=1$ at $T=0$. Our theoretical first-order phase transition result of the S1-1DIS is in good agreement with the result of KH_2PO_4 (KPD) firstly reported by Kittel that one-dimensional system of the KPD carry out a first-order phase transition at $T \neq 0$ [56]. In Figure 3(a2), the total magnetic susceptibility of the FM S1-1DIS has reached a marked peak at T_f and has a broad maximum in the paramagnetic region ($T > T_f$) whereas it monotonously decreases in the second-order case for $D=0$ shown in Figure 2(a2).

The total quadrupolar moment of the FM S1-1DIS is shown in Figure 3(b1). The total quadrupolar moment of the FM S1-1DIS suddenly becomes zero at T_f and then it increases as the temperature increases and it has small changes at high temperature ($T \gg T_f$). One notes that total quadrupolar moment has no phase transition and doesn't become zero except for at T_f whereas the total magnetization becomes zero at $T \geq T_f$. The total quadrupolar moment is $Q_T=1$ at $T=0$, $Q_T=0$ at T_f and $Q_T > 0$ at $T > T_f$. In Figure 3(b2), the total quadrupolar susceptibility of the FM S1-1DIS shows a marked peak at

T_f and becomes zero at $T \geq T_f$. One notes that the broad maximum of the paramagnetic magnetic susceptibility at $T \geq T_f$ in the paramagnetic region results from the quadrupolar moment (Q_T). Because of the M_T and the external magnetic field are zero at $T \geq T_f$. Similarly, quadrupolar susceptibility behavior in the paramagnetic region results from the magnetization (M_T). Because, the total quadrupolar moment ($Q_T \neq 0.0$ at $T \geq T_c$ and T_f) is not zero at $T \geq T_f$.

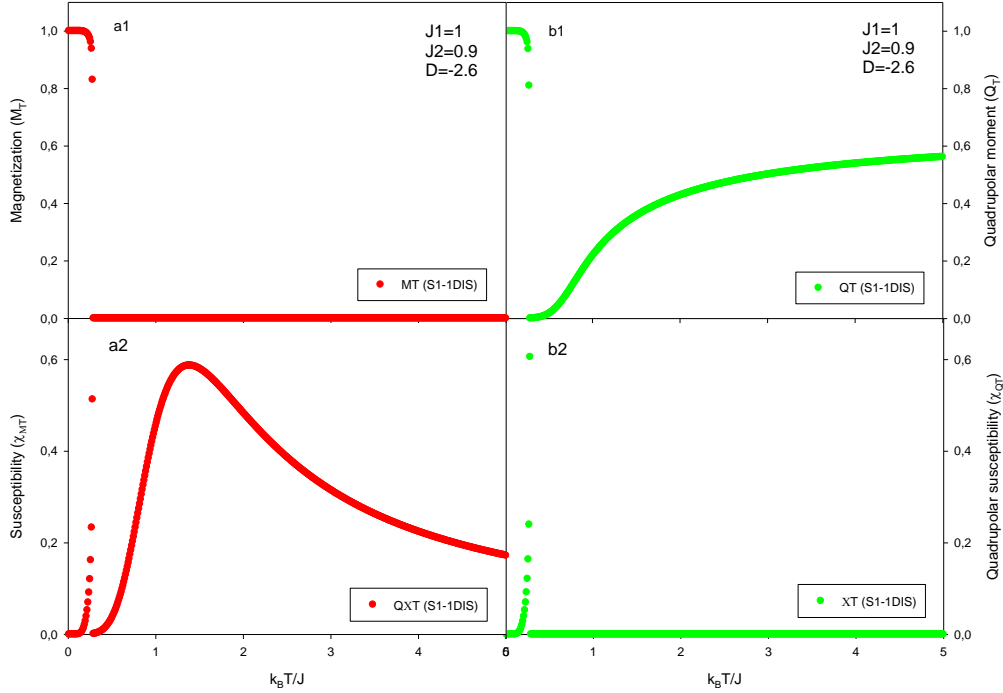


Figure 3. The temperature dependence of the magnetization (a1), susceptibility (a2), quadrupolar moment (b1) and quadrupolar susceptibility (b2) of the S1-1DIS for $J_1=1$, $J_2=0.9$ and $D=-2.6$.

By Figure 4, the applied field dependence of the total magnetization (M_T), total quadrupolar moment (Q_T), total magnetic susceptibility (χ_{MT}) and total quadrupolar susceptibility (χ_{QT}) of the ferromagnetic ($0 < J_1$) S1-1DIS at different temperatures. In Figure 4(a1), the hysteresis curves of the M_T are shown for $D=0$ and at $T=1, 2$ and 3 . The critical field points are $H_c = \pm 0.117$ at $T=1$ and $H_c=0.0$ at $T=2$ and 3 . The hysteresis curves of the S1-1DIS behave wholly superparamagnetic at $T \geq 3$. In Figure 4(a2), the hysteresis curves of the M_T are shown for $D=-2.6$ and at $T=0.05, 0.5$ and 5 . The critical field points are $H_{c1} = \pm 0.214$ and $H_{c2} = \pm 1.504$ at $T=0.05$, $H_{c1} = \pm 0.385$ and $H_{c2} = \pm 0.765$ at $T=2$ and $H_{c1} = H_{c2} = 0.0$ at $T=3$. The hysteresis curves of the S1-1DIS with the first-order phase transition (for $D=-2.6$) exhibit very different behaviors than those of the second-order phase transition (for $D=0$). In Figure 4(b1), the hysteresis curves of the Q_T are shown for $D=0$ and at $T=1, 2$ and 3 . The quadrupolar moment (Q_T) of the S1-1DIS has small two hysteresis loops which are quite different than those of the magnetization (M_T). Since Q_T has no second-order phase transition, it has no critical field points. But Q_T has a minimum value ($Q_T=0.857$) whereas M_T becomes zero at H_c and $T=1$. The hysteresis curves of the Q_T constitute a straight line which is parallel to H-axis (applied field-axis) as the temperature rises ($T \geq 3$) whereas the hysteresis curves of the M_T constitute a straight line with a constant slope. In Figure 4(b2), the hysteresis curves of the Q_T are shown for $D=-2.6$ and at $T=0.05, 0.5$ and 5 . The critical field points are $H_{c1} = \pm 0.214$ and $H_{c2} = \pm 1.504$ at $T=0.05$, $H_{c1} = \pm 0.385$ and $H_{c2} = \pm 0.765$ at $T=2$ and $H_{c1} = H_{c2} = 0.0$ at $T=3$. One notes that $Q_T=0.216$ whereas $M_T=0.0$ at $H_c=0.0$. The theoretical hysteresis findings of FM S1-1DIS are parallel to the findings of single-chain magnets in one-dimensional $[\text{MnR}_4\text{TPP}][\text{TCNE}]$ compounds by Balanda *et al* [59] and one-dimensional polymeric $[\text{Mn}^{\text{III}}(\text{salen})\text{N}_3]$ and $[\text{Mn}^{\text{III}}(\text{salen})\text{Ag}(\text{CN})_2]$ complexes by Panja *et al* [60].

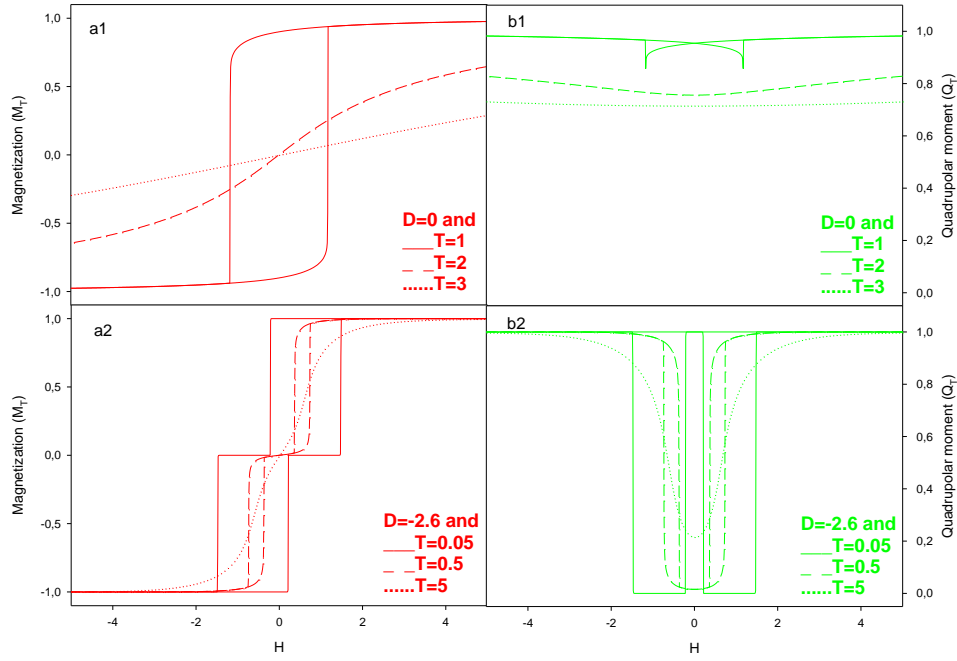


Figure 4. The applied field dependence of the magnetization (a1) for $J_1=1$, $J_2=0.9$, $D=0$, $T=1, 2$, and 3 , the magnetization (a2) for $J_1=1$, $J_2=0.9$, $D=-2.6$, $T=0.05, 0.5$, and 5 , quadrupolar moment (b1) for $J_1=1$, $J_2=0.9$, $D=0$, $T=1, 2$, and 3 , quadrupolar moment (b2) for $J_1=1$, $J_2=0.9$, $D=-2.6$, $T=0.05, 0.5$, and 5 .

In summary, we have examined the temperature and applied field dependence of the magnetization and quadrupolar moment of the S1-1DIS by using Kaneyoshi approach within the EFT. We found that;

- S1-1DIS has a first-or second order phase transition according to the crystal field;
- the magnetization of the S1-1DIS has a second-order phase transition for $D=0$ whereas the quadrupolar moment has no phase transition at T_c ;
- the magnetization of the S1-1DIS has a first-order phase transition for $D=-2.6$ at T_f but the quadrupolar moment has phase transition at T_f and it increases as the temperature increases ($T \geq T_f$);
- paramagnetic magnetic susceptibility decreases monotonically at $T \geq T_c$ whereas it has a broad maximum at $T \geq T_f$. Because of the $M_T=0.0$ at $T \geq T_c$ and T_f , we suggest that susceptibility behaviors in the paramagnetic region result from the quadrupolar moment;
- Similarly, paramagnetic quadrupolar susceptibility result from the magnetization (due to $Q_T \neq 0.0$ at $T \geq T_c$ and T_f);
- hysteresis behaviors of the S1-1DIS with first-order phase transition are quite different than those of the second-order phase transition.

Namely, in the second-order case the S1-1DIS has one critical field point whereas it has two different critical field points in the first-order case. In other word, in the first-order case the S1-1DIS has two distinct hysteresis loops whereas it has one hysteresis loop in the second-order case. Moreover, hysteresis curves of the M_T constitute a straight line with a constant slope. But, hysteresis curves of the Q_T constitute a straight line which is parallel to the applied field-axis as the temperature increases. Therefore, we suggest that hysteresis curves of the Q_T are independent from the applied field and they have a constant value at high temperature. On the other hand, the slope of the hysteresis curves of the M_T decreases as the temperature rises and they become zero at high temperature. Moreover, similar to the spin1/2 -1DIS [41], the nearest-neighbor exchange interaction (J_2) is very important to obtain phase transition in 1DIS (j_2 should be $J_2 > 0$ and $j_2 < j_1$).

References

- [1] T. Kaneyoshi, "Differential operator technique in the Ising spin systems," *Acta Phys. Pol., A* 83, 703-738, 1993.
- [2] T. Kaneyoshi, "Magnetizations of a nanoparticle described by the transverse Ising model," *J. Magn. Magn. Mater.*, 321, 3430-3435, 2009.
- [3] T. Kaneyoshi, "Ferrimagnetic magnetizations of transverse Ising thin films with diluted surfaces," *J. Magn. Magn. Mater.*, 321, 3630-3636, 2009.
- [4] T. Kaneyoshi, "Magnetizations of a transverse Ising nanowire," *J. Magn. Magn. Mater.*, 322, 3410-3415, 2010.
- [5] T. Kaneyoshi, "Phase diagrams of a transverse Ising nanowire," *J. Magn. Magn. Mater.*, 322, 3014-3018, 2010.
- [6] T. Kaneyoshi, "Clear distinctions between ferromagnetic and ferrimagnetic behaviors in a cylindrical Ising nanowire (or nanotube)," *J. Magn. Magn. Mater.*, 323, 2483-2486, 2011.
- [7] T. Kaneyoshi, "Some characteristic properties of initial susceptibility in a Ising nanotube," *J. Magn. Magn. Mater.*, 323, 1145-1151, 2011.
- [8] T. Kaneyoshi, "Ferrimagnetism in a ultra-thin decorated Ising film," *J. Magn. Magn. Mater.*, 336, 8-13, 2013.
- [9] T. Kaneyoshi, "Reentrant phenomena in a transverse Ising nanowire (or nanotube) with a diluted surface: Effects of interlayer coupling at the surface," *J. Magn. Magn. Mater.*, 339, 151-156, 2013.
- [10] T. Kaneyoshi, "Ferrimagnetic magnetizations in a thin film described by the transverse Ising model," *Phys. Status Solidi (b)*, 246, 2359-2365, 2009.
- [11] T. Kaneyoshi, "Magnetic properties of a cylindrical Ising nanowire (or nanotube)," *Phys. Status Solidi (b)*, 248, 250-258, 2011.
- [12] T. Kaneyoshi, "Phase diagrams of a cylindrical transverse Ising ferrimagnetic nanotube; Effects of surface dilution," *Solid State Commun.*, 151, 1528-1532, 2011.
- [13] T. Kaneyoshi, "The possibility of a compensation point induced by a transverse field in transverse Ising nanoparticles with a negative core-shell coupling," *Solid State Commun.*, 152, 883-886, 2012.
- [14] T. Kaneyoshi, "Ferrimagnetism in a decorated Ising nanowire," *Phys. Lett. A*, 376, 2352-2356, 2012.
- [15] T. Kaneyoshi, "The effects of surface dilution on magnetic properties in a transverse Ising nanowire," *Physica A*, 391, 3616-3628, 2012.
- [16] T. Kaneyoshi, "Phase diagrams in an Ising nanotube (or nanowire) with a diluted surface; Effects of interlayer coupling at the surface," *Physica A*, 392, 2406-2414, 2013.
- [17] T. Kaneyoshi, "Characteristic phenomena in nanoscaled transverse Ising thin films with diluted surfaces," *Physica B*, 407, 4358-4364, 2012.
- [18] T. Kaneyoshi, "Phase diagrams in a ultra-thin transverse Ising film with bond or site dilution at surfaces," *Physica B*, 414, 72-77, 2013.
- [19] T. Kaneyoshi, "Characteristic behaviors in an ultrathin Ising film with site- (or bond-) dilution at the surfaces," *Physica B*, 436, 208-214, 2014.
- [20] T. Kaneyoshi, "Unconventional magnetic properties in transverse Ising nanoislands: Effects of interlayer coupling," *Physica E*, 65, 100-105, 2015.
- [21] W. Jiang, X. X. Li, L. M. Liu, J. N. Chen and F. Zhang, "Hysteresis loop of a cubic nanowire in the presence of the crystal field and the transverse field," *J. Magn. Magn. Mater.*, 353, 90-98, 2014.
- [22] W. Jiang, X. X. Li and L. M. Liu, "Surface effects on a multilayer and multisublattice cubic nanowire with core/shell," *Physica E*, 53, 29-35, 2013.
- [23] M. Ertaş and Y. Kocakaplan, "Dynamic behaviors of the hexagonal Ising nanowire," *Phys. Lett. A*, 378, 845-850, 2014.
- [24] Y. Kocakaplan, E. Kantar and M. Keskin, "Hysteresis loops and compensation behavior of cylindrical transverse spin-1 Ising nanowire with the crystal field within effective-field theory based on a probability distribution technique," *Eur. Phys. J. B.*, 86, 420, 2013.
- [25] S. Bouhou, I. Essaoudi, A. Ainane, M. Saber, R. Ahuja and F. Dujardin, "Phase diagrams of diluted transverse Ising nanowire," *J. Magn. Magn. Mater.*, 336, 75-82, 2013.
- [26] A. Zaim, M. Kerouad and M. Boughrara, "Effects of the random field on the magnetic behavior of nanowires with core/shell morphology," *J. Magn. Magn. Mater.*, 331, 37-44, 2013.
- [27] N. Şarlı and M. Keskin, "Two distinct magnetic susceptibility peaks and magnetic reversal events in a cylindrical core/shell spin-1 Ising nanowire," *Solid State Commun.*, 152, 354-359, 2012.
- [28] M. Keskin, N. Şarlı and B. Deviren, "Hysteresis behaviors in a cylindrical Ising nanowire," *Solid State Commun.*, 151, 1025-1030, 2011.
- [29] Y. Yüksel, Ü. Akıncı and H. Polat, "Investigation of bond dilution effects on the magnetic properties of a cylindrical Ising nanowire," *Phys. Status Solidi (b)*, 250, 196-206, 2013.
- [30] Y. Yüksel, Ü. Akıncı and H. Polat, "Investigation of critical phenomena and magnetism in amorphous Ising nanowire in the presence of transverse fields," *Physica A*, 392, 2347-2358, 2013.
- [31] Ü. Akıncı, "Effects of the randomly distributed magnetic field on the phase diagrams of the Ising Nanowire II: Continuous distributions," *J. Magn. Magn. Mater.*, 324, 4237-4244, 2012.

- [32] Ü. Akıncı, "Effects of the randomly distributed magnetic field on the phase diagrams of Ising nanowire I: Discrete distributions," *J. Magn. Magn. Mater.*, 324, 3951-3960, 2012.
- [33] E. Kantar and Y. Kocakaplan, "Hexagonal type Ising nanowire with core/shell structure: The phase diagrams and compensation behaviors," *Solid State Commun.*, 177, 1-6, 2014.
- [34] E. Kantar and M. Keskin, "Thermal and magnetic properties of ternary mixed Ising nanoparticles with core-shell structure: Effective-field theory approach," *J. Magn. Magn. Mater.*, 349, 165-172, 2014.
- [35] E. Kantar, B. Deviren and M. Keskin, "Magnetic properties of mixed Ising nanoparticles with core-shell structure," *Eur. Phys. J. B*, 86, 253, 2013.
- [36] H. Magoussi, A. Zaim and M. Kerouad, "Effects of the trimodal random field on the magnetic properties of a spin-1 Ising nanotube," *Chinese Phys. B*, 22, 116401, 2013.
- [37] N. Şarlı, "Band structure of the susceptibility, internal energy and specific heat in a mixed core/shell Ising nanotube," *Physica B*, 411, 12-25, 2013.
- [38] C. D. Wang and R. G. Ma, "Force induced phase transition of honeycomb-structured ferroelectric thin film," *Physica A*, 392, 3570-3577, 2013.
- [39] N. Şarlı, "Paramagnetic atom number and paramagnetic critical pressure of the sc, bcc and fcc Ising nanolattices," *J. Magn. Magn. Mater.*, 374, 238-244, 2015.
- [40] N. Şarlı, S. Akbudak and M. R. Ellialtıođlu, "The peak effect (PE) region of the antiferromagnetic two-layer Ising nanographene," *Physica B*, 452, 18-22, 2014.
- [41] N. Şarlı, "The effects of next nearest-neighbor exchange interaction on the magnetic properties in the one-dimensional Ising system," *Physica E*, 63, 324-328, 2014.
- [42] N. Bhattacharya and A. R. Chowdhury, "Statistical mechanics of a one-dimensional ferromagnetic chain with an impurity under an external field," *Phys. Rev. B*, 49, 647, 1994.
- [43] M. E. Zhitomirsky and A. Honecker, "Magnetocaloric effect in one-dimensional antiferromagnets," *J. Stat. Mech.*, P07012, 2004.
- [44] G. Ismail and S. Hassan, "Metastability of Ising spin chains with nearest-neighbour and next-nearest-neighbour interactions in random fields," *Chinese Phys.*, 11, 948-954, 2002.
- [45] M. G. Pini and A. Rettori, "Effect of antiferromagnetic exchange interactions on the Glauber dynamics of one-dimensional Ising models," *Phys. Rev. B*, 76, 064407, 2007.
- [46] S. Ares, J. A. Cuesta, A. Sanchez, and R. Toral, "Apparent phase transitions in finite one-dimensional sine-Gordon lattices" *Phys. Rev. E*, 67, 046108, 2003.
- [47] S. T. Chui, and J. D. Weeks, "Pinning and roughening of one-dimensional models of interfaces and steps," *Phys. Rev. B*, 23, 2438-2445, 1981.
- [48] T. W. Burkhardt, "Localisation-delocalisation transition in a solid-on-solid model with a pinning potential," *J. Phys. A: Math. and Gen.*, 14, L63-L68, 1981.
- [49] T. Dauxois, and M. Peyrard, "Entropy-driven transition in a one-dimensional system," *Phys. Rev. E*, 51, 4027-4040, 1995.
- [50] T. Dauxois, N. Theodorakopoulos, and M. Peyrard, "Thermodynamic Instabilities in One Dimension: Correlations, Scaling and Solitons," *J. Stat. Phys.*, 107 (3-4), 869-891, 2002.
- [51] L. van Hove, "Sur l'integrale de configuration pour les systemes de particules a une dimension," *Physica*, 16, 137-143, 1950.
- [52] E. H. Lieb, and D. C. Mattis, *Mathematical Physics in One Dimension*. London: Academic Press, 1966, pp. 25-108.
- [53] D. Ruelle, *Statistical Mechanics: Rigorous Results*. London: Imperial College Press, 1989, pp. 108-143.
- [54] F. J. Dyson, "Existence of a phase-transition in a one-dimensional Ising ferromagnet," *Comm. Math. Phys.*, 12 (2), 91-107, 1969.
- [55] L. D. Landau, and E. M. Lifshitz, *Statistical Physics, Part I*. New York: Pergamon, 1980, pp. 171-179.
- [56] C. Kittel, "Phase Transition of a Molecular Zipper," *Am. J. Phys.*, 37, 917-920, 1969.
- [57] T. Kaneyoshi, "Spin-glass ordering temperature beyond its mean-field value," *Phys. Rev. B*, 24, 2693-2701, 1981.
- [58] M. Bałanda, "AC Susceptibility Studies of Phase Transitions and Magnetic Relaxation: Conventional, Molecular and Low-Dimensional Magnets," *Acta Phys. Pol. A*, 124, 964-976, 2013.
- [59] M. Bałanda, Z. Tomkowicz, W. Haase, and M. Rams, "Single-chain magnet features in 1D [MnR₄TPP][TCNE] compounds," *J. Phys.: Conf. Ser.*, 303 (1), 012036, 2011.
- [60] A. Panja, N. Shaikh, P. Vojtisek, S. Gao, and P. Banerjee, "Synthesis, crystal structures and magnetic properties of 1D polymeric [Mn^{III}(salen)N₃] and [Mn^{III}(salen)Ag(CN)₂] complexes," *New J. Chem.*, 26, 1025-1028, 2002.